

On the stabilization of the most amplified Görtler vortex on a concave surface by spanwise oscillations

By IOANNIS GALIONIS AND PHILIP HALL

Department of Mathematics, Imperial College, London SW7 2AZ

(Received 10 March 2004 and in revised form 26 October 2004)

In the present work the effect of spanwise oscillations on the most unstable Görtler vortex is studied. The wavenumber of the most unstable disturbance is very large, so that the parabolic character of the problem is eliminated. After the disturbances are expanded in a Fourier series in time, the eigenvalue problem is solved for various amplitudes and frequencies of the oscillation. Due to numerical difficulties the treatment of very high amplitudes and/or very low frequencies becomes prohibitively expensive. Therefore an approximate formulation was developed for high magnitudes of the spanwise speed of the oscillation E . The results, which were obtained in all cases, indicate that the disturbances move away from the wall in a logarithmic way, reducing the effects of the oscillation. Consequently, it is impossible to stabilize the flow completely. However, it is shown that a large reduction of the growth rate can be achieved even for moderate values of E .

1. Introduction

One route to transition, especially in aeronautical applications, is through the growth of Görtler vortices in developing flows over concave surfaces. The problem has many characteristics in common with the centrifugally induced Taylor-vortex instability and was studied theoretically by Görtler (1940). It was shown that although the centrifugal force is stabilizing for two-dimensional disturbances, it can create three-dimensional instability in the form of vortices that are parallel to the main stream. Experimental confirmation followed in Gregory & Walker (1950) who used a ‘china-clay technique’ on the concave flap of a Griffith suction aerofoil. In the initial stages of the study of this problem the parallel flow approximation was made. Hämmerlin (1955) solved the resulting approximate equations in a rigorous way and was able to show that the minimum critical Görtler number occurs at zero wavenumber, which corresponds to an infinite wavelength and which of course was in contrast to experimental results. This discrepancy was attributed to the approximations made in deriving the governing system of equations. Later Hämmerlin (1956) and Smith (1955) included some more terms in the expansions related to the curvature and, in the case of Smith, to the boundary layer growth, and were able to show that the minimum critical Görtler number occurs at non-zero values of the wavenumber.

However Hall (1982, 1983) showed in a mathematically justifiable way that for vortices with wavelength of the same or larger order of magnitude than the boundary layer thickness the parallel-flow approximation is wrong, and that in this case the non-parallel effects associated with boundary growth must be retained in the analysis. This results in a system of PDEs, instead of the ODEs of the previous studies. The

system is parabolic in the streamwise direction and therefore its solution depends on both the initial disturbance and where this is introduced into the flow field. A consequence of this is the absence of a unique stability curve or a unique growth rate. However it can be shown that at high Görtler numbers the local wavenumber a_x and the local Görtler number G_x are related by the following expressions:

$$G_x \sim a_x^{-2}, \quad a_x \ll 1 \quad \text{and} \quad G_x \sim a_x^4, \quad a_x \gg 1.$$

Note also that the modes found by Hall correspond to modes with wavenumber of $O(G^{1/4})$ at high Görtler numbers and they are localized in an asymptotically thin layer in the interior of the flow.

Later on the study was extended to three-dimensional boundary layers of a general form (Hall 1985). It was found that at $\lambda \sim O(Re^{-1/2})$, where λ is a crossflow parameter indicating the ratio of the values of the crossflow to streamwise velocity components and Re is the (large) Reynolds number, a significant change occurs in the structure of the vortices. The vortices become time-dependent and they meander as they develop in the chordwise direction. In addition the orientation of the most dangerous vortex is determined by the vortex lines of the basic flow. In relation to that it was shown that for neutral disturbances of small wavelength, the vortex boundaries locally align themselves to be perpendicular to the vortex lines of the mean flow. At larger values of λ the disturbances develop into centre modes of the Orr–Sommerfeld equation which are rendered unstable by centrifugal effects. Most importantly the results obtained indicated that with the existence of sufficiently strong crossflow, the Görtler vortex instability becomes unimportant relative to Tollmien–Schlichting and crossflow instabilities. Finally it was concluded that in the general case the above problem could be solved in the region $0 < \lambda < O(Re^{-1/8})$, but for the specific case of zero pressure gradient the three-dimensional problem could be reduced to an equivalent two-dimensional one, which lifts the latter constraint.

Further work (Denier, Hall & Seddougui 1991) focused on the receptivity of Görtler vortices in the case of surface roughness. In the process of studying this problem it was found that there is another significant wavenumber regime where the fastest growing spatial Görtler vortices occur. In contrast to the modes found by Hall, these are located in a thin layer next to the wall and their wavenumber scales as $G^{1/5}$. Letting $G \rightarrow \infty$ the parallel flow approximation is valid and the system of governing equations reduce to ODEs. As an extension of this work the effects of a three-dimensional boundary layer were studied by introducing a spanwise flow in Bassom & Hall (1991). A crossflow parameter (λ) was again introduced indicating the ratio of the size of the crossflow and the streamwise flow. This parameter becomes important for vortices with $O(1)$ wavenumber in a $G \gg 1$ flow, when it attains an order of magnitude of $O(Re^{-1/2}G^{1/2})$. As the crossflow and wavenumber increase, a mode can be obtained whose structure is dominated by viscous effects. When this happens λ becomes $O(Re^{-1/2}G^{3/5})$ and the large wavenumber is the one studied in the latter work. The results of the linear theory that were obtained indicate that although in the two-dimensional Görtler problem the stationary vortices are essentially unstable, with the existence of sufficiently strong crossflow they can be stabilized.

In the present study we have treated the most unstable Görtler vortices in the case of a concave wall that is oscillating in the spanwise direction. This has been extensively suggested as a means of suppressing turbulence (Kwing-So-Choi 2002; Kwing-So-Choi, DeBisschop & Clayton 1998; Nikitin 2000; Quadio & Ricco 2003). The control of turbulence by spanwise oscillations is achieved by the destruction or modification of the streamwise vortex structures embedded in the turbulent flow. Here our concern is

whether such a control mechanism can significantly modify the growth rates of the most dangerous form of linear instability associated with streamwise vortices. Our calculations focus on the initial stages of transition on a concave surface and suggest that the introduction of this kind of three-dimensionality can significantly reduce the growth rate of the unstable (in the two-dimensional case) Görtler vortices, but can never stabilize them completely. This is due to the fact that, though the effects of the oscillation become important as the amplitude of the speed of the oscillations is increased, at the same time the disturbances move away from the wall, reducing the influence of the oscillations. Specifically it is shown that for a range of wavenumbers around the one corresponding to the most unstable mode the vortices remain unstable even for large oscillation amplitudes.

The procedure adopted in the rest of this paper is as follows: In §2 the mean flow and the instability problems are formulated. In §3 we explain the numerical approach used to solve the disturbance problem and give some results. In §4 we give an asymptotic formulation for the case of large values of the magnitude of the oscillations. Finally in §5 we draw some conclusions.

2. Derivation of the equations

The flow under investigation is taken to be incompressible, and the kinematic viscosity and the density are denoted by ν_∞^* and ρ_∞^* respectively. Furthermore there are two ‘velocities’ in this problem: the velocity of the fluid at infinity U_∞^* which we use as our velocity reference scale and the amplitude of the spanwise velocity of the wall ϵ^* . The reference length can be defined arbitrarily, say L^* . The characteristic time scale to be used is $t_{ref} = L^*/U_\infty^*$. Finally a combination of the reference density and velocity can produce a reference pressure. Hence if quantities denoted by an asterisk are dimensional, the non-dimensional stretched quantities are given as follows:

$$\begin{aligned} (u^+, v^+, w^+) &= (u^*, Re^{1/2}v^*, Re^{1/2}w^*)/U_\infty^*, & \epsilon &= \epsilon^*/U_\infty^*, \\ (x, y, z) &= (x^*, Re^{1/2}y^*, Re^{1/2}z^*)/L^*, \\ t &= t^*U_\infty^*/L^*, & p^+ &= \frac{p^*}{\rho_\infty^*U_\infty^{*2}}, \end{aligned}$$

where

$$Re = \frac{U_\infty^*L^*}{\nu_\infty^*}.$$

The non-dimensional form of the Navier–Stokes equations is

$$\left. \begin{aligned} u_x^+ + v_y^+ + w_z^+ &= 0, \\ u_t^+ + u^+u_x^+ + v^+u_y^+ + w^+u_z^+ &= -p_x^+ + Re^{-1}u_{xx}^+ + u_{yy}^+ + u_{zz}^+, \\ v_t^+ + u^+v_x^+ + v^+v_y^+ + w^+v_z^+ &= -Re p_y^+ + Re^{-1}v_{xx}^+ + v_{yy}^+ + v_{zz}^+, \\ w_t^+ + u^+w_x^+ + v^+w_y^+ + w^+w_z^+ &= -Re p_z^+ + Re^{-1}w_{xx}^+ + w_{yy}^+ + w_{zz}^+. \end{aligned} \right\} \quad (1)$$

The spanwise velocity of the wall, whose shape is defined by $y = g(x)$, now becomes $w_{wall}^+ = \epsilon \cos(\omega t)$, ω being the non-dimensional angular frequency of the oscillation: $\omega = \omega^*L^*/U_\infty^*$. We assume flow quantities can be written as a superposition of a mean part corresponding to an undisturbed flow and a small fluctuating part that describes the disturbances. We write

$$\left. \begin{aligned} p^+ &= \bar{p}(x) + \Delta Re^{-1/2} \tilde{p}(x, y, z) + O(\Delta^2), \\ (u^+, v^+, w^+) &= (\bar{u}, \bar{v}, \bar{w}) + \Delta(\tilde{u}, \tilde{v}, \tilde{w}) + O(\Delta^2), \end{aligned} \right\} \quad (2)$$

where Δ is a small curvature parameter. Substituting these expansions into equations (1), separating the terms that are coefficients of different powers of Δ , taking into account that the undisturbed flow does not vary in z and making the Prandtl transformation of dependent and independent variables:

$$y \rightarrow y - g(x), \quad \bar{v} \rightarrow \bar{v} + g'\bar{u}, \quad \tilde{v} \rightarrow \tilde{v} + g'\tilde{u},$$

equations (1) become:

continuity equation

$$\left. \begin{aligned} \bar{u}_x + \bar{v}_y &= 0, \\ \tilde{u}_x + \tilde{v}_y + \tilde{w}_z &= 0, \end{aligned} \right\} \quad (3)$$

x -momentum equation

$$\left. \begin{aligned} \bar{u}_t + \bar{u}\bar{u}_x + \bar{v}\bar{u}_y &= -\bar{p}_x + \bar{u}_{yy}, \\ \tilde{u}_t + \bar{u}\tilde{u}_x + \bar{u}_x\tilde{u} + \bar{v}\tilde{u}_y + \bar{u}_y\tilde{v} + \bar{w}\tilde{u}_z &= \Delta_2\tilde{u}, \end{aligned} \right\} \quad (4)$$

y -momentum equation

$$\left. \begin{aligned} \bar{p}_y &= 0, \\ \tilde{v}_t + \bar{u}\tilde{v}_x + \bar{v}_x\tilde{u} + \bar{v}\tilde{v}_y + \bar{v}_y\tilde{v} + \bar{w}\tilde{v}_z + G\chi(x)\bar{u}\tilde{u} &= -\bar{p}_y + \Delta_2\tilde{v}, \end{aligned} \right\} \quad (5)$$

z -momentum equation

$$\left. \begin{aligned} \bar{w}_t + \bar{u}\bar{w}_x + \bar{v}\bar{w}_y &= \bar{w}_{yy}, \\ \tilde{w}_t + \bar{u}\tilde{w}_x + \bar{w}_x\tilde{u} + \bar{v}\tilde{w}_y + \bar{w}_y\tilde{v} + \bar{w}\tilde{w}_z &= -\bar{p}_z + \Delta_2\tilde{w}, \end{aligned} \right\} \quad (6)$$

where $\Delta_2 = \partial^2/\partial y^2 + \partial^2/\partial z^2$ and $G\chi(x) = 2d^2g/dx^2$. Since the reference velocity is $U_\infty^* = \bar{u}(y \rightarrow \infty)$, the boundary conditions appropriate to these equations are the following:

$$\left. \begin{aligned} \text{at } y = 0: \quad \bar{u} = \bar{v} = 0, \quad \bar{w} = \epsilon \cos(\omega t), \quad \tilde{u} = \tilde{v} = \tilde{w} = 0, \\ \text{as } y \rightarrow \infty: \quad \bar{u} \rightarrow 1, \quad \bar{w} \rightarrow 0, \quad \tilde{u}, \tilde{v}, \tilde{w} \rightarrow 0. \end{aligned} \right\} \quad (7)$$

In the above, the disturbance equations can be Fourier transformed in z to give continuity equation

$$u_x + v_y + ikw = 0, \quad (8)$$

x -momentum equation

$$u_t + \bar{u}u_x + \bar{u}_xu + \bar{v}u_y + \bar{u}_yv + ik\bar{w}u = u_{yy} - k^2u, \quad (9)$$

y -momentum equation

$$v_t + \bar{u}v_x + \bar{v}_xu + \bar{v}v_y + \bar{v}_yv + ik\bar{w}v + G\chi(x)\bar{u}u = -p_y + v_{yy} - k^2v, \quad (10)$$

z -momentum equation

$$w_t + \bar{u}w_x + \bar{w}_xu + \bar{v}w_y + \bar{w}_yv + ik\bar{w}w = -ikp + w_{yy} - k^2w, \quad (11)$$

with the following boundary conditions:

$$\text{at } y = 0 : u = v = w = 0, \quad \text{as } y \rightarrow \infty : u, v, w \rightarrow 0. \quad (12)$$

It can be seen that the equations of the mean flow concerning the streamwise and vertical components of the velocity do not contain any dependence on the spanwise velocity component, the time derivatives can be dropped and consequently the basic flow equations can be reduced to the Blasius boundary layer equations.

In accordance with Denier *et al.* (1991, hereafter referred to as DHS), the most amplified Görtler vortex lies in a region a distance $k^{-1} \propto G^{-1/5}$ from the wall. In this region $\Psi = ky$ is of $O(1)$. Taking into account equation (6) and demanding the effects of \bar{w} and the time changes remain in the equation, we are led to the substitution $\hat{\tau} = G^{2/5}t$. Using the new y -coordinate and time we find

$$\frac{\partial \bar{w}}{\partial \hat{\tau}} + \frac{\bar{u}}{G^{2/5}} \frac{\partial \bar{w}}{\partial x} + \frac{k\bar{v}}{G^{2/5}} \frac{\partial \bar{w}}{\partial \Psi} = \frac{k^2}{G^{2/5}} \frac{\partial^2 \bar{w}}{\partial \Psi^2}.$$

Taking the limit $G^{1/5} = k/\bar{\lambda} \rightarrow \infty, \bar{\lambda} \sim O(1)$, the following equation is obtained, which as can be seen, does not depend on the streamwise and vertical components of the velocity:

$$\frac{\partial \bar{w}}{\partial \hat{\tau}} = \bar{\lambda}^2 \frac{\partial^2 \bar{w}}{\partial \Psi^2}. \tag{13}$$

The solution of this equation must remain bounded as $\Psi \rightarrow \infty$ and must satisfy the boundary condition related to the spanwise velocity component on the wall. Hence we have

$$\bar{w}(\Psi, \hat{\tau}) = \epsilon e^{-\Phi} \cos(\hat{\omega}\hat{\tau} - \Phi),$$

with $\Phi = \sqrt{\frac{1}{2}\hat{\omega}\Psi/\bar{\lambda}}$.

As far as the disturbance equations are concerned, we observe that the x -momentum equation contains only terms related to u and v . Furthermore it is evident that p and w disturbances appear in equations (8) and (11) on their own, and therefore they can be easily expressed in terms of u and v only. The aim is to reduce equations (8), (10) and (11) to one equation containing only u and v . The final result is the following:

$$\begin{aligned} & \left(\bar{u}_{xyy} + k^2\bar{v}_y + k^4 + ik^3\bar{w} + ik\bar{w}_{yy} + k^2 \frac{\partial}{\partial \hat{\tau}} \right) v + \bar{v}_x u_{yy} \\ & + (\bar{u}_{xyy} + k^2\bar{v}_x + k^2 G \chi(x)\bar{u} + 2ik\bar{w}_{xy})u + \left(\bar{u}_{yy} + k^2\bar{u} - \bar{u} \frac{\partial^2}{\partial y^2} \right) v_x \\ & + 2 \left(\bar{u}_{xy} + \bar{u}_x \frac{\partial}{\partial y} \right) u_x + v_{yyyy} - \bar{v} v_{yyy} - \left(\bar{v}_y + 2k^2 + \frac{\partial}{\partial \hat{\tau}} + ik\bar{w} \right) v_{yy} \\ & + (\bar{u}_{xy} + k^2\bar{v})v_y + 2ik\bar{w}_x u_y = 0. \end{aligned} \tag{14}$$

Equations (9) and (14) are quite general, since no assumption was made regarding the form of the mean flow. They can be manipulated even further by taking into account the characteristics of the mean flow, which is the Blasius flow in this case. Near the wall we have that $\bar{u} = \mu(x)y$, where μ is the shear stress on the wall and is known to have the form

$$\mu(x) = 0.4696x^{-1/2}/\sqrt{2}.$$

Hence in the disturbance equation we make the following substitutions:

$$\bar{u}_x = -\bar{v}_y = \mu_x y, \quad \bar{u}_y = \mu, \quad \bar{u}_{xy} = \mu_x, \quad \bar{u}_{yy} = 0, \quad \bar{u}_{xxy} = \mu_{xx}, \quad \bar{u}_{xyy} = 0, \tag{15}$$

where the second equality in the first relation can be deduced from the continuity equation for the mean flow. Furthermore we observe that since \bar{w} is independent of x then $\bar{w}_x = \bar{w}_{xy} = 0$. Finally in the region of interest it can be shown that the appropriate expansions of the disturbance quantities based on a WKB approach are

the following:

$$\left. \begin{aligned} u(x, y, t) &= \exp\left(G^{3/5} \int \beta(x) dx\right) (u_0(y, t) + G^{-1/5} u_1(y, t) + \dots), \\ v(x, y, t) &= G^{2/5} \exp\left(G^{3/5} \int \beta(x) dx\right) (v_0(y, t) + G^{-1/5} v_1(y, t) + \dots). \end{aligned} \right\} \quad (16)$$

Substituting the above into the disturbance equations, considering only the first terms of the expansions (16), setting $y = \Psi/k$, $t = \hat{t}/G^{2/5}$, with $\bar{w} = G^{1/5} \hat{w}$ with $\hat{w} = O(1)$ we obtain

$$\left(\frac{\partial^2}{\partial \Psi^2} - 1 - \frac{1}{\bar{\lambda}^2} \frac{\partial}{\partial \hat{t}} - \frac{\beta G^{3/5} \mu \Psi}{k^3} - \frac{\mu \Psi}{k^3} \frac{\partial}{\partial x} - \frac{\mu_x \Psi}{k^3} - \frac{\bar{v}}{k} \frac{\partial}{\partial \Psi} - \frac{i \hat{w}}{\bar{\lambda}}\right) u_0 = \frac{\mu G^{2/5}}{k^2} v_0 \quad (17)$$

and

$$\begin{aligned} &\left[k^4 G^{2/5} \left(1 + \frac{i \hat{w}}{\bar{\lambda}} + \frac{1}{\bar{\lambda}^2} \frac{\partial}{\partial \hat{t}} - \frac{\mu_x \Psi}{k^3} + \frac{i \hat{w}_{\Psi \Psi}}{\bar{\lambda}}\right) + \frac{G \mu \Psi \beta}{k} \left(k^2 - k^2 \frac{\partial^2}{\partial \Psi^2}\right)\right] v_0 \\ &\quad + \bar{v}_x k^2 u_{0 \Psi \Psi} + (\mu_{xx} + k^2 \bar{v}_x + k G \chi \mu \Psi) u_0 + 2 \mu_x \beta G^{3/5} \left(1 + \Psi \frac{\partial}{\partial \Psi}\right) u_0 \\ &\quad + G^{2/5} \left[k^4 v_{0 \Psi \Psi \Psi \Psi} - \bar{v} k^3 v_{0 \Psi \Psi \Psi} - \left(k^2 \frac{1}{\bar{\lambda}^2} \frac{\partial}{\partial \hat{t}} + \frac{i k^2 \hat{w}}{\bar{\lambda}} + 2k^2 - \frac{\mu_x \Psi}{k}\right) k^2 v_{0 \Psi \Psi}\right. \\ &\quad \left. + (\mu_x + k^2 \bar{v}) k v_{0 \Psi}\right] = 0. \end{aligned} \quad (18)$$

Setting $k = \bar{\lambda} G^{1/5}$ and taking the limit $G \rightarrow \infty$ gives

$$\left(\frac{\partial^2}{\partial \Psi^2} - 1 - \frac{1}{\bar{\lambda}^2} \frac{\partial}{\partial \hat{t}} - \frac{\beta \mu \Psi}{\bar{\lambda}^3} - \frac{i \hat{w}}{\bar{\lambda}}\right) u_0 = \frac{\mu}{\bar{\lambda}^2} v_0, \quad (19)$$

and

$$\left[\left(\frac{\partial^2}{\partial \Psi^2} - 1 - \frac{1}{\bar{\lambda}^2} \frac{\partial}{\partial \hat{t}} - \frac{\beta \mu \Psi}{\bar{\lambda}^3} - \frac{i \hat{w}}{\bar{\lambda}}\right) \left(\frac{\partial^2}{\partial \Psi^2} - 1\right) + \frac{i}{\bar{\lambda}^3} \frac{\partial \hat{w}}{\partial \hat{t}}\right] v_0 = -\frac{\chi \mu \Psi}{\bar{\lambda}^3} u_0, \quad (20)$$

where we have replaced $\hat{w}_{\Psi \Psi}$ with $\hat{w}_{\hat{t}}/\bar{\lambda}^2$. Finally for computational purposes we write $\bar{\lambda} = (\chi \mu^2)^{1/5} \tilde{\lambda}$, $\beta = (\chi^3 \mu)^{1/5} \tilde{\beta}$, $\hat{t} = \epsilon G^{-1/5} = (\chi \mu^2)^{1/5} E$, $u_0 = \mu U_0$, $v_0 = (\chi \mu^2)^{2/5} V_0$, $\hat{w} = (\chi \mu^2)^{2/5} \Omega$ and $\hat{t} = \bar{\lambda}^{-2} \tau$. The final eigenvalue problem to be solved is

$$\begin{aligned} &\left(\frac{\partial^2}{\partial \Psi^2} - 1 - \frac{\tilde{\beta}}{\tilde{\lambda}^3} \Psi - \frac{\partial}{\partial \tau} - \frac{i \hat{w}}{\tilde{\lambda}}\right) U_0 = \frac{1}{\tilde{\lambda}^2} V_0 \\ &\left[\left(\frac{\partial^2}{\partial \Psi^2} - 1 - \frac{\tilde{\beta}}{\tilde{\lambda}^3} \Psi - \frac{\partial}{\partial \tau} - \frac{i \hat{w}}{\tilde{\lambda}}\right) \left(\frac{\partial^2}{\partial \Psi^2} - 1\right) + \frac{i \hat{w}_{\tau}}{\tilde{\lambda}}\right] V_0 = -\frac{\Psi}{\tilde{\lambda}^3} U_0 \end{aligned} \quad (21)$$

with the following boundary conditions:

$$\text{at } y = 0: \quad U_0 = V_0 = V_{0 \Psi} = 0, \quad \text{as } y \rightarrow \infty: \quad U_0, V_0, V_{0 \Psi} \rightarrow 0, \quad (22)$$

where now: $\hat{w}(\Psi, \tau) = E \exp(-\sqrt{\frac{1}{2} \Omega \Psi / \tilde{\lambda}}) \cos((\Omega / \tilde{\lambda}^2) \tau - \sqrt{\frac{1}{2} \Omega \Psi / \tilde{\lambda}})$.

3. Numerical solution of the eigenvalue problem

3.1. Formulation

Since the basic flow is periodic with respect to $\Omega\tau/\tilde{\lambda}^2$ we write

$$U_0(\Psi, \tau) = \sum_{m=-\infty}^{+\infty} \tilde{U}_{0m}(\Psi) e^{im\Omega\tau/\tilde{\lambda}^2}, \quad (23)$$

together with a similar expression for V_0 . \hat{w} can be expressed as

$$\hat{w}(\Psi, \tau) = \sum_{n=-1}^1 A_n(\Psi) e^{in\Omega\tau/\tilde{\lambda}^2}, \quad (24)$$

where $A_{\pm 1}(\Psi) = \frac{1}{2}E \exp[-(1 \pm i)\sqrt{\frac{1}{2}\Omega\Psi/\tilde{\lambda}}]$ and $A_0 \equiv 0$. Equations (21) become

$$\begin{aligned} & \sum_m \left(\frac{d^2 \tilde{U}_{0m}}{d\Psi^2} e^{im\Omega\tau/\tilde{\lambda}^2} \right) - \sum_m \left[\left(\frac{\tilde{\beta}\Psi}{\tilde{\lambda}^3} + 1 \right) \tilde{U}_{0m} e^{im\Omega\tau/\tilde{\lambda}^2} \right] \\ & - \frac{i}{\tilde{\lambda}} \sum_n A_n e^{in\Omega\tau/\tilde{\lambda}^2} \sum_m \tilde{U}_{0m} e^{im\Omega\tau/\tilde{\lambda}^2} - \frac{1}{\tilde{\lambda}^2} \sum_m im\Omega \tilde{U}_{0m} e^{im\Omega\tau/\tilde{\lambda}^2} = \frac{1}{\tilde{\lambda}^2} \sum_m \tilde{V}_{0m} e^{im\Omega\tau/\tilde{\lambda}^2}, \end{aligned}$$

where for brevity the range of the indices has been omitted. Note also that more detail of the analysis given in this section can be found in the thesis of Gallionis (2003). We can deduce from above that

$$-\frac{i}{\tilde{\lambda}} A_1 \tilde{U}_{0(m-1)} + D \tilde{U}_{0m} - \frac{i}{\tilde{\lambda}} A_{-1} \tilde{U}_{0(m+1)} = \frac{1}{\tilde{\lambda}^2} \tilde{V}_{0m}, \quad (25)$$

where

$$D = \frac{d^2}{d\Psi^2} - \left(\frac{\tilde{\beta}\Psi}{\tilde{\lambda}^3} + 1 + \frac{im\Omega}{\tilde{\lambda}^2} \right).$$

This equation is valid for all values of $m \in (-\infty, +\infty)$. However numerically, one has to truncate this series to a finite range, say $[-M, M]$.

As far as the second disturbance equation is concerned, it can be seen that the operator between the first brackets on the left-hand side of is the same as the operator of the first disturbance equation, and therefore it leads to similar terms, when it operates on the term $(d^2 V_0/d\Psi^2 - V_0)$. We also find that

$$\hat{w}_\tau V_0 = - \sum_m \frac{i\Omega}{\tilde{\lambda}^2} A_{-1} \tilde{V}_{0(m+1)} e^{im\Omega\tau/\tilde{\lambda}^2} + \sum_m \frac{i\Omega}{\tilde{\lambda}^2} A_1 \tilde{V}_{0(m-1)} e^{im\Omega\tau/\tilde{\lambda}^2}.$$

Therefore

$$\begin{aligned} & -\frac{i}{\tilde{\lambda}} A_1 \left(\frac{d^2}{d\Psi^2} - 1 - \frac{i\Omega}{\tilde{\lambda}^2} \right) \tilde{V}_{0(m-1)} + D \left(\frac{d^2}{d\Psi^2} - 1 \right) \tilde{V}_{0m} \\ & - \frac{i}{\tilde{\lambda}} A_{-1} \left(\frac{d^2}{d\Psi^2} - 1 + \frac{i\Omega}{\tilde{\lambda}^2} \right) \tilde{V}_{0(m+1)} = -\frac{\Psi}{\tilde{\lambda}^3} \tilde{U}_{0m}. \quad (26) \end{aligned}$$

Equations (25) and (26) together with appropriate boundary conditions specify an eigenvalue problem for the spatial growth rate. The equations can be put into the

simpler form

$$\left. \begin{aligned} -\frac{i}{\tilde{\lambda}} A_1 \tilde{U}_{0(m-1)} + D_m \tilde{U}_{0m} - \frac{i}{\tilde{\lambda}} A_{-1} \tilde{U}_{0(m+1)} - \frac{1}{\tilde{\lambda}^2} \tilde{V}_{0m} &= \tilde{\beta} \frac{\Psi}{\tilde{\lambda}^3} \tilde{U}_{0m}, \\ \frac{\Psi}{\tilde{\lambda}^3} \tilde{U}_{0m} - \frac{i}{\tilde{\lambda}} A_1 D_1 \tilde{V}_{0(m-1)} + D_m D_0 \tilde{V}_{0m} - \frac{i}{\tilde{\lambda}} A_{-1} D_{-1} \tilde{V}_{0(m+1)} &= \tilde{\beta} \frac{\Psi}{\tilde{\lambda}^3} D_0 \tilde{V}_{0m}, \end{aligned} \right\} \quad (27)$$

where

$$D_m = \frac{d^2}{d\Psi^2} - 1 - \frac{im\Omega}{\tilde{\lambda}^2}.$$

It can be seen from equations (22) that the boundary conditions appropriate to \tilde{U}_{0m} and \tilde{V}_{0m} are the following:

$$\left. \begin{aligned} \text{at } y = 0, m \in [-M, M]: \quad \tilde{U}_{0m} = \tilde{V}_{0m} = \tilde{V}_{0m\Psi} = 0; \\ \text{as } y \rightarrow \infty, m \in [-M, M]: \quad \tilde{U}_{0m}, \tilde{V}_{0m}, \tilde{V}_{0m\Psi} \rightarrow 0. \end{aligned} \right\} \quad (28)$$

The above equations have been discretized using a spectral collocation scheme along the normal direction. The resulting linear eigenvalue problem has been solved using the Implicitly Restarted Arnoldi Method. (See Lehoucq, Sorensen & Yang (1998) for a discussion of the method.) The eigenvalue with the largest real part corresponds to the most unstable Görtler vortex.

3.2. Results

A series of tests was performed for various values of the frequency of the oscillations Ω (ranging from 0.1 to 5) and the amplitude of the oscillations E (ranging from 0.5 to 5000). It was observed during these runs that the required number of modes increases with increasing E and with decreasing Ω . For instance converged results could be achieved with only 5 modes ($M = 2$) for the case $\Omega = 0.5$, $E = 3$, but at least 41 modes ($M = 20$) were required for the case $\Omega = 0.1$, $E = 10$, or $\Omega = 2.5$, $E = 1000$, since the modes around the 'steady' mode $m = 0$ are still important, as figure 1 reveals for the case $\Omega = 3.25$ and $E = 2000$. This introduced a practical difficulty and no results were obtained using equations (27) for a small Ω and/or large E .

Figure 2 shows the dependence of the most unstable eigenvalue $\tilde{\beta}$ on various combinations of Ω and E . It can be seen that $\tilde{\beta}$ is a monotonically decreasing function of E , that is the vortices become less unstable with increasing maximum speed of the oscillation. However no negative value of $\tilde{\beta}$ could be achieved for the cases that were studied.

Figure 3 is a slice of the previous figure along the dashed line corresponding to $\Omega = 3.25$. It can be seen that at frequencies of this order of magnitude the growth rate decreases rapidly with E till about $E \sim 100$ and then starts levelling off. In particular for the same decrease of $\tilde{\beta}$ achieved between $E = 0$ and $E = 100$, we have to increase the amplitude to $E = 1000$.

Furthermore figures 4–6 illustrate the real and the imaginary part of the eigenvectors for the cases $E = 160, 200$ and 1000 respectively, when $\Omega = 3.25$ and at time $\tau = 0$. All the eigenvectors were normalized so that the largest value of the imaginary part of U_0 is unity. These plots show that with the increase of E the disturbances move progressively away from the wall and therefore their characteristics become less and less dependent on the value of E . This is in agreement with the trend of $\tilde{\beta}$. This observation was used in order to make the study of the problem for values of $E \gtrsim 2500$ practical. The boundary conditions for $\Psi = 0$ were imposed at $\Psi = \sqrt{2/\Omega} \log(E/2500)$ which is the value of Ψ at which the amplitude of the oscillation becomes $O(10^{-3})$.

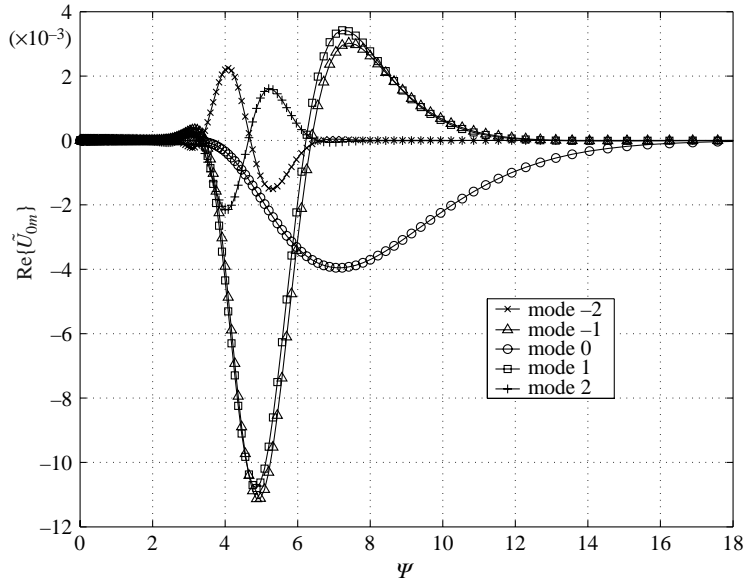


FIGURE 1. The real part of \tilde{U}_{0m} for $-2 \leq m \leq 2$ for the $\Omega = 3.25$ and $E = 2000$ case. It can be seen that these modes are still important and accurate solution can be obtained with a much higher number of modes.

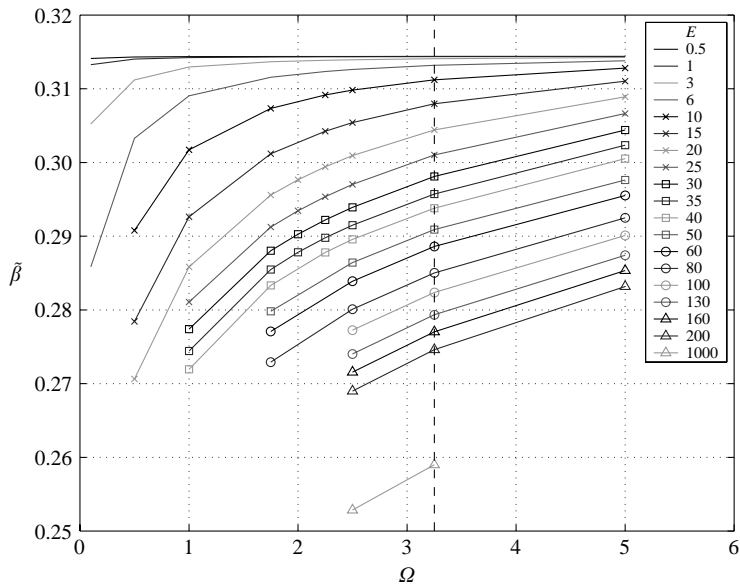


FIGURE 2. The dependence of the growth rate of the most amplified Görtler vortex on the (velocity) amplitude E and frequency Ω of the oscillation of the wall.

Since the magnitude of the disturbances would anyway be very small closer to the wall, this should not produce much error in the solution.

Results were obtained for the case of $E = 5000$, $\Omega = 3.25$ for both the complete domain and the reduced domain. In both cases the wavenumber of the most unstable vortex was 0.49 and its growth rate was 0.246. Because of numerical difficulties the

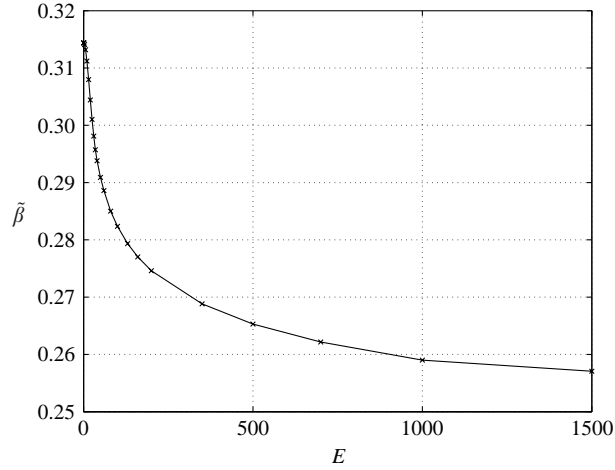


FIGURE 3. The dependence of the growth rate of the most amplified Görtler vortex on the (velocity) amplitude E for $\Omega = 3.25$. This figure is a slice of figure 2 along the $\Omega = 3.25$ line.

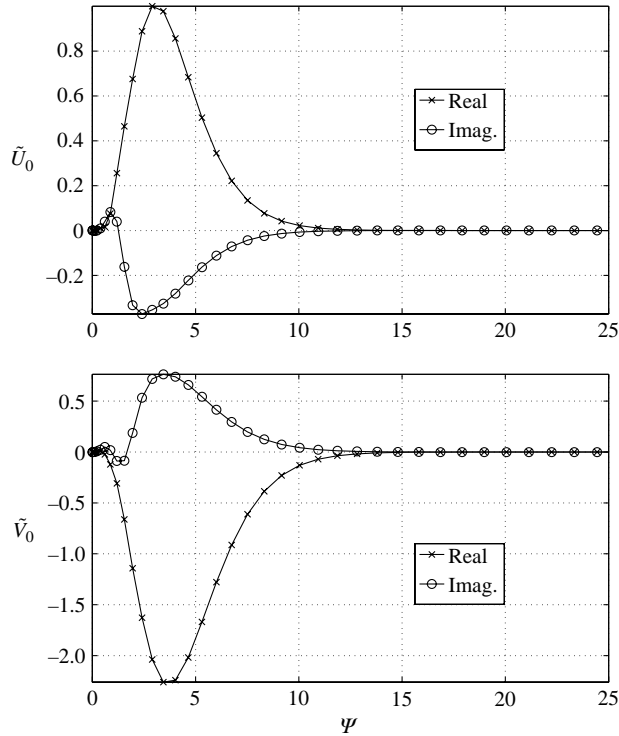


FIGURE 4. The real and imaginary parts of the \tilde{U}_0 and \tilde{V}_0 disturbances of the most amplified Görtler vortex for the case $E = 160$, $\Omega = 3.25$.

values of the growth rate cannot be calculated with a precision of more than 3 decimal digits and of the wavenumber with more than 2. The eigenvectors for these cases can be seen in figures 7 and 8. It can be seen that the two results are in good agreement and the approximation mentioned above should produce accurate results also for larger E . Unfortunately no accurate results could be obtained for even higher

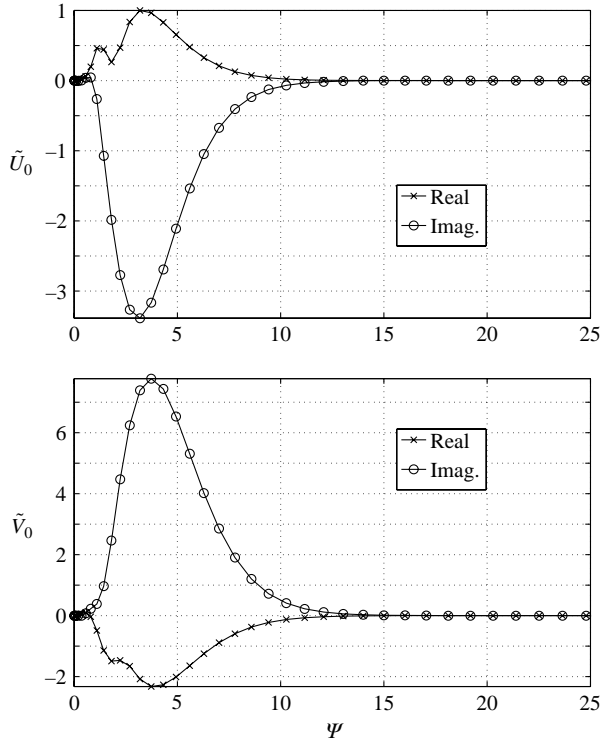


FIGURE 5. The real and imaginary parts of the \tilde{U}_0 and \tilde{V}_0 disturbances of the most amplified Görtler vortex for the case $E = 200$, $\Omega = 3.25$.

values of E ($E > 10^4$). However it is possible to develop an asymptotic approximation for $E \gg 1$; and this is done in the following section.

4. Asymptotics for the case $E \gg 1$

4.1. Formulation

We see from the graphs of the solutions of the previous section that as E is increased, the disturbances move away from the wall at a rate that is approximately logarithmic in E . This could be anticipated from the form of the operator:

$$\mathcal{K} = \frac{\partial^2}{\partial \Psi^2} - 1 - \frac{\tilde{\beta}\Psi}{\tilde{\lambda}^3} - \frac{\partial}{\partial \tau} - \frac{iE}{\tilde{\lambda}} \exp\left(-\sqrt{\frac{\Omega}{2}} \frac{\Psi}{\tilde{\lambda}}\right) \cos \alpha,$$

where

$$\alpha = \frac{\Omega}{\tilde{\lambda}^2} \tau - \sqrt{\frac{\Omega}{2}} \frac{\Psi}{\tilde{\lambda}}.$$

In the region of interest, where the magnitude of the disturbances is large, the order of each of the terms has to be the same, in this case $O(1)$. The appropriate scalings are found to be

$$\begin{aligned} \Psi &= (\log E)^{5(1-d)/4} + \chi, & \tilde{\lambda} &= (\log E)^{(1-d)/4} \lambda_0, & \tilde{\beta} &= (\log E)^{-(1-d)/2} \beta_0, \\ \Omega &= (\log E)^{2d} \Omega_0, & U_0 &= U_{00}, & V_0 &= (\log E)^{(1-d)/2} V_{00}. \end{aligned}$$

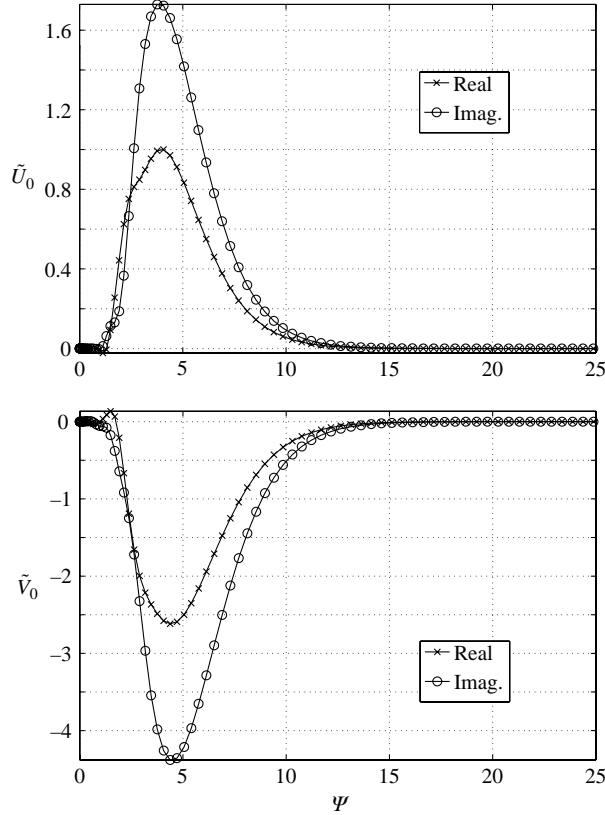


FIGURE 6. The real and imaginary parts of the \tilde{U}_0 and \tilde{V}_0 disturbances of the most amplified Görtler vortex for the case $E = 1000$, $\Omega = 3.25$.

Here the constant d will be fixed at a later stage. With these stretchings the term of \mathcal{H} that contains the exponential becomes

$$\frac{E}{(\log E)^{(1-d)/4}} \exp \left[-(\log E) \sqrt{\frac{\Omega_0}{2}} \frac{1}{\tilde{\lambda}_0} \right] \exp \left[-(\log E)^{(5d-1)/4} \sqrt{\frac{\Omega_0}{2}} \frac{\chi}{\tilde{\lambda}_0} \right].$$

The second exponential contains the effects of the oscillation (Stokes layer). The only possible value of d that will make this term independent of $(\log E)$ is $d = 1/5$. Thus the new eigenvalue problem can be formulated as follows:

$$\left. \begin{aligned} \left(\frac{\partial^2}{\partial \chi^2} - 1 - \frac{\tilde{\beta}_0}{\tilde{\lambda}_0^3} - \frac{\partial}{\partial \tau} - \frac{i\hat{w}_0}{\tilde{\lambda}_0} \right) U_{00} &= \frac{1}{\tilde{\lambda}_0^2} V_{00}, \\ \left[\left(\frac{\partial^2}{\partial \chi^2} - 1 - \frac{\tilde{\beta}_0}{\tilde{\lambda}_0^3} - \frac{\partial}{\partial \tau} - \frac{i\hat{w}_0}{\tilde{\lambda}_0} \right) \left(\frac{\partial^2}{\partial \chi^2} - 1 \right) + \frac{i\hat{w}_{0\tau}}{\tilde{\lambda}_0} \right] V_{00} &= -\frac{1}{\tilde{\lambda}_0^3} U_{00}, \end{aligned} \right\} \quad (29)$$

and

$$\hat{w}_0(\chi, \tau) = \exp \left(-\sqrt{\frac{\Omega_0}{2}} \frac{\chi}{\tilde{\lambda}_0} \right) \cos \left(\frac{\Omega_0}{\tilde{\lambda}_0^2} \tau - \sqrt{\frac{\Omega_0}{2}} \frac{\chi}{\tilde{\lambda}_0} \right).$$

The boundary conditions as $\chi \rightarrow -\infty$ are the following: $U_{00}, V_{00}, V_{00\chi} \rightarrow 0$. As $\chi \rightarrow \infty$ the \hat{w}_0 terms become negligible and the above equations can be written as a single

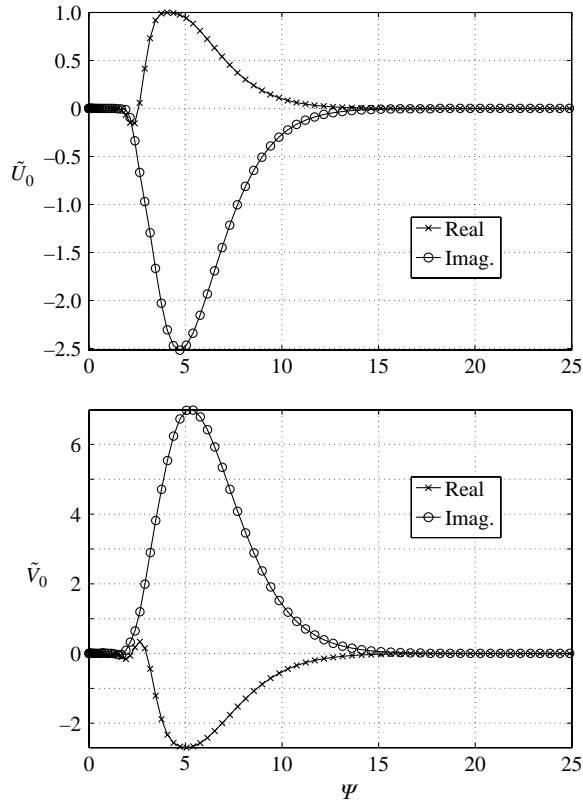


FIGURE 7. The real and imaginary parts of the \tilde{U}_0 and \tilde{V}_0 disturbances of the most amplified Görtler vortex for the case $E = 5000$, $\Omega = 3.25$.

equation with constant coefficients. However the equation has only two exponentially decaying solutions so we cannot make the disturbance go to zero directly in this region, since at infinity the solution is still oscillatory. Instead we must find a solution in a larger region using a WKB method. Full details can be found in the thesis of Galionis; we will give only the most important details here.

If we return to the original equations (21), make the same stretching of parameters and variables except for Ψ , for which we now set $\Psi = (\log E)\eta$, and focus on the region $\eta > 1$ we obtain a pair of equations which can be combined to give a single equation for U_{00} . For simplicity we set $\delta = (\log E)^{-2}$, $\sigma = \beta_0 \lambda_0^{-3}$, $R = \lambda_0^{-5}$, $D = d/d\eta$ and $U_{00} \equiv U$. Thus

$$[\delta^3 D^6 - \delta^2(3 + 2\sigma\eta)D^4 - \delta^2(3\sigma)D^3 + \delta(\sigma^2\eta^2 + 4\sigma\eta + 3)D^2 + \delta\sigma(\sigma\eta + 3)D + \eta R - (1 + \sigma\eta)^2]U = 0. \quad (30)$$

Equation (30) lends itself to a WKBJ solution. It can be shown that equation (30) has a turning point in the region $\eta > 1$, let us say at $\eta = \eta_t$. For $1 < \eta < \eta_t$ the behaviour of U is oscillatory and for $\eta > \eta_t$ monotonic. These two expressions for U can be matched by the study of the intermediate layer in the vicinity of the turning point. Setting

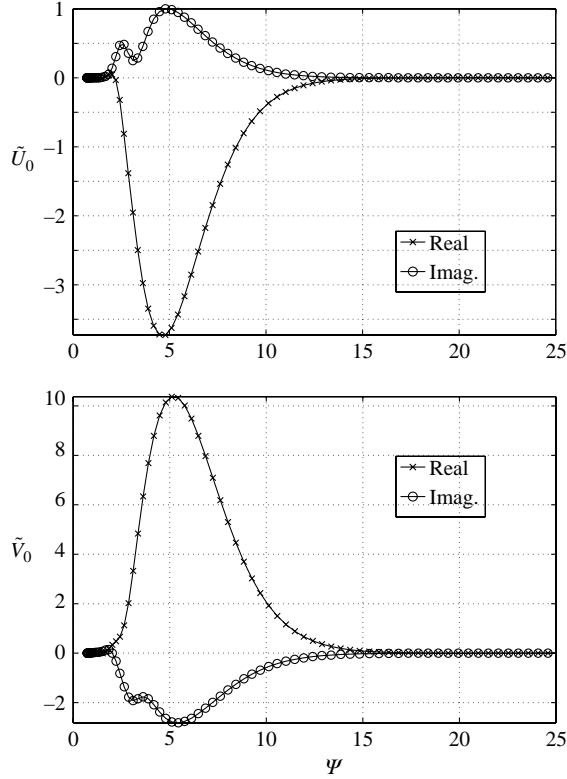


FIGURE 8. The real and imaginary parts of the \tilde{U}_0 and \tilde{V}_0 disturbances of the most amplified Görtler vortex for the case $E = 5000$, $\Omega = 3.25$ (reduced domain).

$\eta - \eta_t = \delta^{1/6}\xi$ and $\gamma = \sqrt{R^2 - 4\sigma R/[(\sigma\eta_t + 1)(\sigma\eta + 3)]} > 0$, we obtain the following:

$$\left. \begin{aligned} U_{osc} &\sim C'_1 \delta^{-1/24} (-\xi)^{-1/4} \sin \left[\frac{2}{3} \delta^{-1/4} \gamma^{1/2} (-\xi)^{3/2} + \phi \right], \\ U_{int} &\sim K_1 \text{Ai}(\gamma^{1/3} \delta^{-1/6} \xi), \\ U_{mon} &\sim C_1 \delta^{-1/24} \xi^{-1/4} \exp \left[-\frac{2}{3} \delta^{-1/4} \gamma^{1/2} \xi^{3/2} \right]. \end{aligned} \right\} \quad (31)$$

Matching the above with the corresponding forms either side of the turning point yields the argument of the sine in the oscillatory part of U . This matches with the oscillatory solution for $U_{00}(\chi)$ mentioned before. This yields a behavioural boundary condition for $U_{00}(\chi)$ and $V_{00}(\chi)$ as $\chi \rightarrow \infty$. Numerically this behavioural boundary condition has to be replaced with a numerical one on the upper limit of a truncated domain $\chi_{max} \gg 1$; namely

$$\begin{aligned} \frac{dU_{00}}{d\chi} + \kappa U_{00} &= 0 \quad \text{and} \quad \frac{dV_{00}}{d\chi} + \kappa V_{00} = 0, \\ \kappa &= -q_0 \frac{\cos(q_0 \chi_{max}) - N \sin(q_0 \chi_{max})}{\sin(q_0 \chi_{max}) + N \cos(q_0 \chi_{max})}, \end{aligned}$$

where q_0 is the real solution of the auxillary equation associated with the constant-coefficient equation corresponding to (29) and valid as $\chi \rightarrow \infty$, and N is a quantity whose form is derived by the matching of the oscillating and solutions $U_{osc}(\eta)$ and $U_{00}(\chi)$. The eigenvalue problem to be solved is given by equations (29)

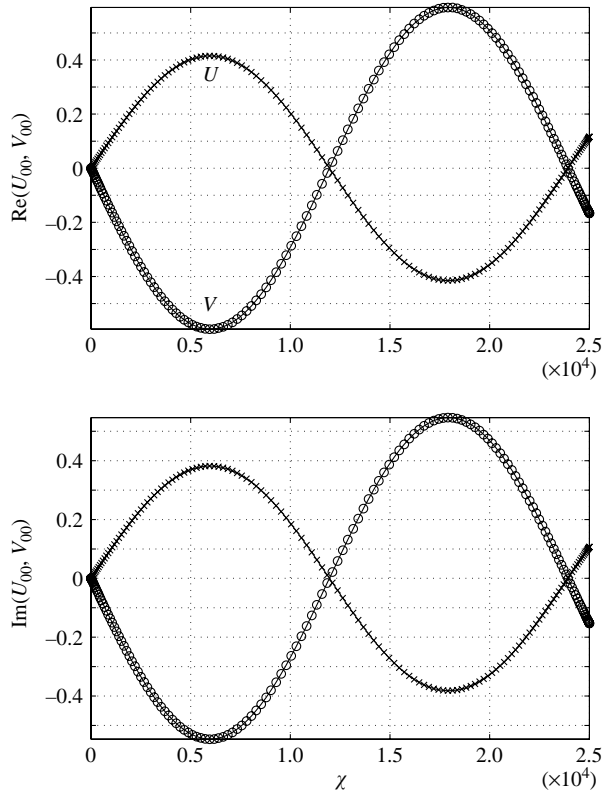


FIGURE 9. The real and imaginary parts of the U_{00} and V_{00} disturbances of the most amplified Görtler vortex for the case $\log E = 10^{11}$, $\Omega_0 = 1$.

with exponentially decaying solutions as $\chi \rightarrow -\infty$ and the aforementioned periodic conditions as $\chi \rightarrow \infty$.

4.2. Asymptotic results

Our calculations showed that for $\log E \geq 10^{11}$ the maximum growth rate and the wavenumber at which the latter is achieved are practically constant. The results taken for $\log E = 10^{11}$ are the following: $\beta_0 \approx 0.5823559$ at $\lambda_0 = 0.4882989$. The U_{00} and V_{00} disturbances under these conditions are illustrated in figure 9. It is evident that the eigenfunctions decay rapidly to zero for negative values of χ due to the effects of the Stokes layer and over the largest part of the domain the solutions are oscillatory with wavenumber q_0 . It should also be mentioned that the above results were calculated for $M = 2$, i.e. 5 modes were kept. Except for the zeroth mode these have very small amplitudes and attain non-zero values in practice over a very small region: $-5 \leq \chi \leq 10$, as is illustrated in figure 10. The aforementioned results were obtained with $\Omega_0 = 1$, but they are valid for other values of the frequency parameter. Indeed the small extent and influence of the other modes relative to the zeroth mode explains the observed minimal effect of the frequency Ω_0 on β_0 and λ_0 .

The numerical results indicate that the quantity $\partial\beta_0/\partial\lambda_0$ is very small over a large range of values of λ_0 . This means in practice that the numerical results should be accurate as far as the maximum growth rate β_0 is concerned, but they might yield a poor approximation to λ_0 . Indeed, if we set $E = 5000$, we obtain $\log E \approx 8.5172$ and

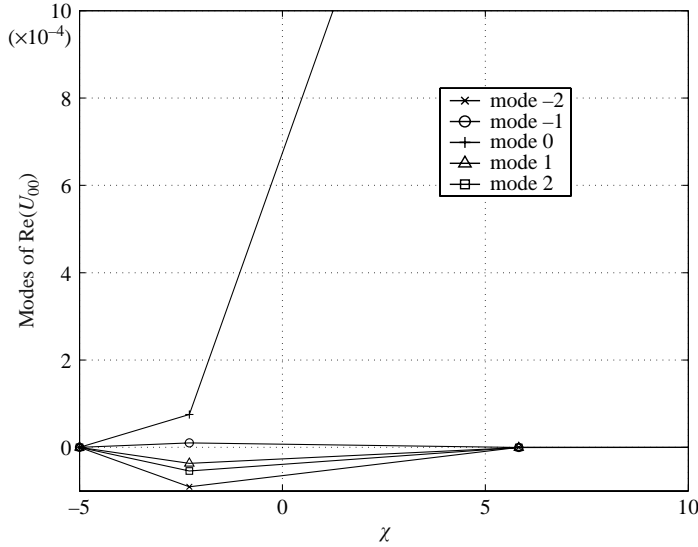


FIGURE 10. The real part of the modes of U_{00} with $(-2 \leq m \leq 2)$ for the most amplified Görtler vortex case with $\log E = 10^{11}$, $\Omega_0 = 1$.

subsequently

$$\begin{aligned} \Omega &= (\log E)^{2/5} \Omega_0 \approx 2.356, \\ \tilde{\beta} &= (\log E)^{-2/5} \beta_0 \approx 0.237, \\ \tilde{\lambda} &= (\log E)^{1/5} \lambda_0 \approx 0.749. \end{aligned}$$

The results obtained from the original problem (equations (27), (28)) were $\tilde{\beta} = 0.246$ and $\tilde{\lambda} = 0.48$ for the most unstable vortex at the same value of Ω . The asymptotic value of $\tilde{\beta}$ is very close to the one obtained from the original problem although the value of E is very small. On the other hand the wavenumber of the most unstable Görtler vortex is poor. The agreement of the asymptotic and original problem results might be better if the value of E used in the original problem were larger. However the fact remains that $\beta = (\log E)^{(-2/5)} \beta_0 > 0$, indicating that although a stabilization of some Görtler vortices can be achieved with large E , the instability in general remains in the small wavelengths around $\lambda = (\log E)^{1/5} \lambda_0$. The values of the amplitude relevant for the validity of the asymptotic structure found above are well beyond the range of physical relevance but we feel it is important to show the structure since it confirms that complete stabilization of centrifugally induced vortices is impossible at large amplitudes.

5. Conclusions

A study concerning the most unstable Görtler vortex has been carried out in the case of a spanwise oscillating concave surface. It has been shown that these spanwise oscillations reduce the growth rate of the most unstable vortex, but without reaching negative values, even when very large values of the magnitude of the speed of oscillation E are used. The reason behind this is the fact that as E is increased the disturbances move towards the interior of the flow and therefore the influence of the motion of the wall is reduced. This is seen by the logarithmic behaviour of both

the spanwise wavenumber $\tilde{\lambda}$ and the growth rate $\tilde{\beta}$ of the most unstable mode when $E \gg 1$.

Unfortunately the study of the case of very small frequency of oscillation Ω combined with very large values of E cannot be treated due to numerical difficulties. It has been observed however that the growth rate is more sensitive to changes of Ω than of E . Indeed even for relatively moderate values of E but small values of Ω it was seen that the maximum growth rate was reduced substantially.

For the dimensional values of the quantities related to the oscillations (E and Ω) the following can be derived:

$$E = \hat{\epsilon}(\chi\mu^2)^{-1/5},$$

where

$$\hat{\epsilon} = \frac{Re^{1/2}}{U_\infty^* G^{1/5}} \epsilon^*, \quad \chi G = 2Re^{1/2} L^* \frac{d^2 g^*}{dx^{*2}}, \quad \mu = \left. \frac{du^*}{dy^*} \right|_0 \frac{L^*}{U_\infty^*} \frac{1}{Re^{1/2}}.$$

Substituting these in the above relation for E and taking into account the expression for the Reynolds number, we derive an expression for the dimensional magnitude of the spanwise velocity of the oscillation ϵ^* :

$$\epsilon^* = 2^{1/5} \nu_\infty^{*3/5} [g^{*''} (u_w^{*'})^2]^{1/5} E.$$

Similarly for the dimensional frequency of the oscillation we obtain

$$\omega^* = 2^{2/5} \nu_\infty^{*1/5} [g^{*''} (u_w^{*'})^2]^{2/5} \Omega.$$

In order to get an idea of the order of magnitude of these quantities we set $\nu^* \sim 10^{-5} \text{ m}^2 \text{ s}^{-1}$, $g^{*''} \sim 10^{-2} \text{ m}^{-1}$ and $u_w^{*' } = (0.4969/\sqrt{2}) \sqrt{U_\infty^{*3}/\nu_\infty^* x^*} \text{ s}^{-1}$ in a Blasius boundary layer. Therefore

$$\epsilon^* \sim 10^{-3} \left(\frac{U_\infty^*}{x^*} \right)^{1/5} E \quad \text{and} \quad \omega^* \sim \left(\frac{U_\infty^*}{x^*} \right)^{2/5} \Omega,$$

where U_∞^* has units m s^{-1} , ϵ^* and x^* have units m and ω^* has units s^{-1} . As was seen in the previous results, a satisfactory decrease of the growth rate ($\sim -15\%$) of the most dangerous mode can be achieved for $E = 500$ and $\Omega = 3.25$. According to the above expressions this means

$$\epsilon^* \sim \left(\frac{U_\infty^*}{x^*} \right)^{1/5} \quad \text{and} \quad \omega^* \sim \left(\frac{U_\infty^*}{x^*} \right)^{2/5}.$$

Figure 11 shows the values of the quantity $(U_\infty^*/x^*)^{1/5}$ for various combinations of U_∞^* and x^* that are expected in aeronautical applications taking into account that we have to remain in the incompressible speed region, i.e. $10 \leq U_\infty^* \leq 60 \text{ m s}^{-1}$ and $1 \leq x^* \leq 5 \text{ m}$. This figure reveals that both ϵ^* and ω^* are practically always of order 1 m s^{-1} and 1 s^{-1} respectively.

Viewing the above relations from a different perspective, one can arrive at the conclusion that for a specific magnitude and frequency of the oscillations and increasing speed, it becomes harder to reduce the growth rate of the dangerous modes, since E and Ω are inversely proportional to $(U_\infty^*)^{1/5}$ and $(U_\infty^*)^{2/5}$ respectively and the stabilizing effects become important for large values of E . On the other hand Ω becomes smaller, which is beneficial for the stabilization, but as was shown above, in practice it remains within a specified region of values of order 1.

Moreover an interesting effect is that for $E \gg 1$ and $\Omega \sim O(1)$, the solution becomes independent of Ω at zeroth-order accuracy. Taking into account that Ω determines

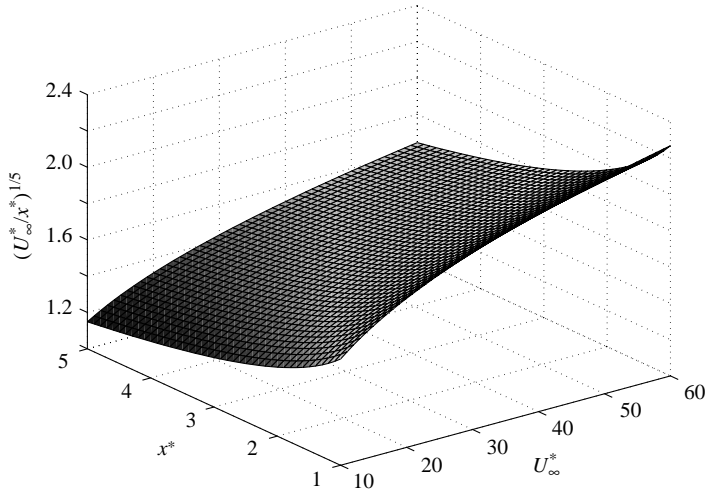


FIGURE 11. The dependence of the quantity $(U_\infty^*/x^*)^{1/5}$ for various combinations of U_∞^* and x^* .

with E the extent of the Stokes layer according to the equation for \hat{w} , the above conclusion should not come as a surprise, since at $E \gg 1$ the Stokes layer will be very wide, no matter what the value of Ω , as long as the latter remains of order 1.

Finally it should be pointed out that since the vortices move away from the wall for increasing E , there will be a point at which they will be located far enough from the wall and towards the upper limit of the boundary layer, where a different flow structure is valid. This indicates the need for some further work, in order to be able to conclude firmly whether the most unstable Görtler vortices can be stabilized or not.

REFERENCES

- BASSOM, A. P. & HALL, P. 1991 Vortex instabilities in three-dimensional boundary layers: the relationship between Görtler and crossflow vortices. *J. Fluid Mech.* **232**, 647–680.
- BENDER, C. M. & ORSZAG, S. A. 1978 *Advanced Mathematical Methods for Scientists and Engineers*. McGraw-Hill.
- CHANDRASEKHAR, S. 1981 *Hydrodynamic and Hydromagnetic Stability*, pp. 25–26. Dover.
- DENIER, J. P., HALL, P. & SEDDOUGUI, S. O. 1991 On the receptivity problem for Görtler vortices: vortex motions induced by wall roughness. *Phil. Trans. R. Soc. Lond. A* **335**, 51–85.
- GALIONIS, I. 2003 Instability of some viscous flows. PHD thesis, Imperial College.
- GÖRTLER, H. 1940 Über eine dreidimensionale Instabilität laminarer Grenzschichten an Konkaven Wänden. *Nachr. Ges. Wiss. Göttingen, Math-Phys. Klasse, Neue Folge* **1** **2**, 1–26.
- HALL, P. 1982 Taylor-Görtler vortices in fully developed or boundary-layer flows: linear theory. *J. Fluid Mech.* **124**, 475–494.
- HALL, P. 1983 The linear development of Görtler vortices in growing boundary layers. *J. Fluid Mech.* **130**, 41–58.
- HALL, P. 1985 The Görtler vortex instability mechanism in three-dimensional boundary layers. *Proc. R. Soc. Lond. A* **399**, 135–152.
- HALL, P. 1988 The nonlinear development of Görtler vortices in growing boundary layers. *J. Fluid Mech.* **193**, 243–266.
- HÄMMERLIN, G. 1955 Über das Eigenwertproblem der dreidimensionalen Instabilität laminarer Grenzschichten an konkaven Wänden. *J. Rat. Mech. Anal.* **4**, 279–321.

- HÄMMERLIN, G. 1956 Zur Instabilitätstheorie der ebenen Staupunktströmung. In *50 Jahre Grenzschichtforschung* (ed. H. Görtler & W. Tollmien), pp. 315–327. Vieweg.
- KWING-SO-CHOI 2002 Near-wall structure of turbulent boundary layer with spanwise-wall oscillation. *Phys. Fluids* **14**, 2530–2542.
- KWING-SO-CHOI, DEBISSCHOP, J. R. & CLAYTON, B. R. 1998 Turbulent boundary-layer control by means of spanwise-wall oscillation. *AIAA J.* **36**, 1157–1163.
- LEHOUCQ, R. B., SORENSEN, D. C. & YANG, C. 1998 *ARPACK Users Guide: Solution of Large-scale Eigenvalue Problems with Implicitly Restarted Arnoldi Methods*. SIAM, Philadelphia.
- NIKITIN, N. V. 2000 On the mechanism of turbulence suppression by spanwise surface oscillations. *Fluid Dyn.* **35**, 185–190 (original in *Mekh. Zhid. I Gaza* **35**(2), 37–44, 2000).
- QUARDIO, M. & RICCO, P. 2003 Initial response of a turbulent channel flow to spanwise oscillation of the walls. *J. Turbulence* **4**, paper no. 7, 1–23.
- SMITH, A. M. O. 1955 On the growth of Taylor–Görtler vortices along highly concave walls. *Q. Appl. Maths* **13**, 233–262.